Proceedings of OMAE 2008
ASME 27th International Conference on Offshore Mechanics and Arctic Engineering
June 15-20, 2008, Estoril, PORTUGAL

OMAE2008-57482

FINITE ELEMENT SIMULATIONS AND EXPERIMENTAL INVESTIGATIONS OF SIMPLE 2-D GEOMETRIES IN SLAMMING

Adrian CONSTANTINESCU
ANAST - Naval Architecture, Ocean & Harbour Engineering, Sea & Inland Navigation Technics, Transportation Systems Analysis
University of Liège
Chemin des Chevreuils 1, Liège, Belgium

Alain NEME
LBMS ENSIETA-UBO-ENIB ENSIETA
2 rue François Verny, 29806 Brest Cedex 9
France

Nicolas JACQUES
LBMS ENSIETA-UBO-ENIB ENSIETA
2 rue François Verny, 29806 Brest Cedex 9
France

Philippe RIGO
ANAST - Naval Architecture, Ocean & Harbour Engineering, Sea & Inland Navigation Technics, Transportation Systems Analysis
University of Liège, and FNRS Belgium
Chemin des Chevreuils 1, Liège, Belgium

ABSTRACT

This paper presents a numerical and experimental study of fluid structure interaction during the impact of a solid body on a water surface. The main request is the modeling of the slamming forces acting on the ship structure in severe sea conditions.

The numerical work uses the finite element modeling of a structure impact with free water surface. The first analysis use the commercial finite element code ABAQUS/Standard and combines the assumption of small displacements for the ideal fluid and the solid with an asymptotic formulation for accurate pressure evaluation on the boundary of the wet surface. For deformable strickers, two methods are developed. The first method employs a weak fluid-structure coupling. The second method, more accurate, uses an implicit fluid-structure coupling using a convergence criterion. The second analysis is represented by the simulations of slamming with ABAQUS/Explicit. The simulation uses a viscous, compressible fluid and a soft-exponential law to manage the contact between fluid and solid. The results in term of pressure and total effort applied to the rigid structure are in good agreement with first numerical results and especially with the FLUENT CFD.

In order to validate the numerical methods, slamming experimental tests were carried out with a new hydraulic shock press at the ENSIETA laboratory.

Keywords – slamming, fluid-structure interaction, hydro-elastic analysis, ABAQUS/Explicit, shock press

INTRODUCTION

Since some decades, the slamming phenomenon represents a major difficulty to witch are confronted the naval engineers. Sometimes ships suffer local damage from the impact load or large-scale buckling on the deck. Recent events illustrate the disastrous consequences of slamming. According to ISSC'91 (International Ship and Offshore Structure Congress [1]) during the previous 30 years, the damages due to slamming represent 12% of the total prejudices recorded for mono-hull ships.

The slamming phenomenon implies very large impulsive loads because a considerable mass of water is displaced in a short time. Slamming is particularly important for fast ships because of the increase of ship size and as new concepts has decreased their rigidity. For these ships, the global and local responses must be taken into account for dimensioning.

Concerning the global responses, the whole ship is brutally subjected to a bending moment and shearing force, introducing general vibrations of the beam ship. The local response describes more especially the small repeated impacts on the hull that accelerates the fatigue by local damages. Finally the ship is submitted to local loading, leading to high frequencies vibrations, added to its global response at lower frequency.

Theses responses affect the passengers comfort and more dangerously may threaten the safety of the ship. In these conditions, it is important to predict exactly the applied forces for a correct and optimal design.

Copyright © 2008 by ASME

Slamming is a strongly non-linear and three-dimensional phenomenon, depending on the deadrise angle between body and free water surface. With air trapping the mechanism of impact becomes more complex. According to Langrand [2], the effects generated by the presence of air cannot be neglected for deadrise angles lower than 4° ($\beta \leq 3°$).

V. Bertram [3] gives an overview of the most important analytical approaches of slamming, pointing out that in the end only computational fluid dynamics (CFD) methods are expected to bring considerable progress, while classical theories work.

For our first approach, we focus the analysis on the aspect of hydro-elasticity, limiting the study to simple geometries (2D and pseudo-3D) and 2D flows, as a first step to develop more sophisticated 3D numerical methods.

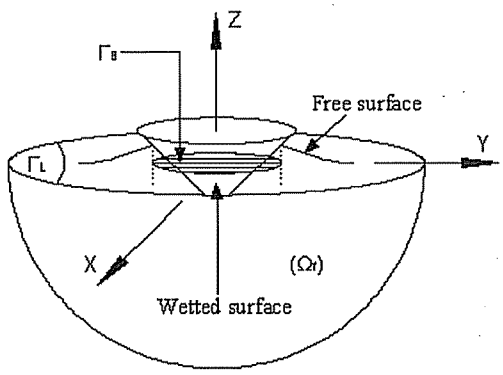

Figure 1 – Geometric definition

II. FIRST APPROACH – ABAQUS/Standard

We consider the problem of impact of a 3-D body on a water surface, Fig. 1. The fluid problem is formulated within potential flow theory for an ideal fluid (incompressible, inviscid, irrotational) initially to the rest. We assume small disturbances both for the fluid and the solid. The flow will be analyzed with eulerian variables and must fulfill the conservation of mass and the momentum equation.

II.A. Mathematical formulation

The velocity vector anywhere in the fluid domain is obtrained as $\mathbf{v} = grad\ \Phi$. The velocity potential $\Phi(x_0,y_0,z_0,t)$ must satisfy the following conditions:

$$\Delta\Phi = 0 \qquad \text{in } \Omega_f \qquad (1)$$

The continuity of the normal speeds between the fluid and solid particles are written by:

$$\mathbf{grad}\ \Phi \cdot \mathbf{n} = \mathbf{V_s} \cdot \mathbf{n} \qquad \text{on the wetted surface} \qquad (2)$$

On the free surface the condition is:

$$\Phi = 0 \qquad \text{on the free surface} \qquad (3)$$

It expresses the condition of zero relative pressure on this surface. A decay condition states that the flow is not disturbed far from the body:

$$\mathbf{grad}\ \Phi \rightarrow 0 \qquad \text{for } \sqrt{\left(x_0^2 + y_0^2 + z_0^2\right)} \rightarrow \infty \qquad (4)$$

The fluid problem is very complex, with non-linear limit conditions. In order to simplify, Wagner [4] proposed to project these limit conditions on the initial water surface ($z_0 = 0$). Within that new configuration, another equation can be written:

$$\frac{\partial\Phi}{\partial z_0} = \frac{\partial h}{\partial t} \text{ where } h = \int_0^t \left.\frac{\partial\Phi}{\partial z_0}\right|_{(x_0,y_0,0,\tau)} d\tau \qquad \text{on } \Gamma_B \qquad (5)$$

Γ_B is vertical projection of the wetted body surface on $z_0 = 0$, Γ_L the liquid free surface projected on $z_0 = 0$ and h the instantaneous draft of the body.

The hydrodynamic pressure is calculated by the non-stationary Bernoulli equation:

$$p = -\rho_f \frac{\partial\Phi}{\partial t} - \rho_f \frac{(\text{grad}\Phi)^2}{2} \qquad (6)$$

The second term (non-linear) represents the steady state dynamic pressure, smaller compared to the first term.

To complete the resolution of the hydrodynamic fluid problem it is necessary to know the extent of the wet surface $d(t)$ (Fig 2). The optimal way is to find the intersection between the free surface rising and the position of the solid body. The free surface elevation is expressed by the integral in time of the normal derivative of the velocity potential. Thus, we can solve the problem of the displacement potential $\Psi=\Psi(x_0,y_0,z_0,t)$ such that:

$$\Psi = \int_0^t \Phi(x_0,y_0,z_0,t)dt \text{ and } h = \left.\frac{\partial\Psi}{\partial z_0}\right|_{(x_0,y_0,0,t)} \qquad (7)$$

The displacement potential is the solution of the following equations system:

$$\Delta\Psi = 0 \qquad \text{in } \Omega_f \qquad (8)$$

$$\frac{\partial\Psi}{\partial z_0} = U_{sz} \qquad \text{on the wetted surface } \Gamma_B \qquad (9)$$

$$\Psi = 0 \qquad \text{on the free surface } \Gamma_L \qquad (10)$$

II.B. Numerical model and particularities

Donguy [5] developed a numerical approach to simulate 3D slamming problems. For solving the fluid problem, he used a fluid-heat analogy under the hypothesis of incompressibility and irrotational initial velocity field for the fluid, considering the velocity potential or the displacement potential like temperature. The finite element code CASTEM was employed to determine the fluid velocity field (heat flux) and solid evolutions.

We have globally followed the same approach using the commercial finite element code ABAQUS associated with PYTHON and FORTRAN languages instead of CASTEM. Some procedures have been modified and several numerical aspects improved. The developed code was generically named Impact++ ABAQUS after Impact++ CASTEM.

The fluid-heat transfer analogy is employed to solve the fluid dynamics problem with finite element code ABAQUS. The heat transfer model is given by the following equations:

Copyright © 2008 by ASME

$$\Delta T = 0 \qquad \text{in } \Omega_f \qquad (11)$$

$$\lambda \frac{\partial T}{\partial z_0} = -\mathbf{q}\cdot\mathbf{z} \qquad \text{on } \Gamma_B \qquad (12)$$

$$\frac{\partial T}{\partial z_0} = \frac{\partial h}{\partial t} \qquad \text{on } \Gamma_L \qquad (13)$$

$$T = 0 \qquad \text{on } \Gamma_L \qquad (14)$$

In eq. (12), **z** stands for the unit vertical vector. An equivalent system to eqs.(1-3) and eq. (5) is obtained if the temperature T is expressed in [m^2/s], the thermal conductivity is set to $\lambda=1$, and **q** = - **v** = - **grad** Φ expressed in [m/s] in the thermal module of ABAQUS/Standard.

For the displacement potential, we use the same system (11-14), but the temperature T will be consequently expressed in [m^2] with thermal conductivity $\lambda=1$ and $\boldsymbol{q}$ in [m].

The calculation of the pressure is associated with an asymptotic development at the wetted surface boundary. The asymptotic study led to the determination of two zones (near-field and far-field) in which two asymptotic developments are obtained and then connected. The composite solution for the pressure includes a far-field solution (fulfilling conditions far from the body-surface intersection, but being singular at the intersection) and a near-field solution (valid in the vicinity of the intersection, describing the formation of a jet). The far-field pressure is approximated by central differencing of the Bernoulli's equation (15).

For the correct evaluation of the resulting total force, it is necessary to consider also the near-field pressure, eq. (16). Since we used numerical resolution and finite distances from the exact wetted surface boundary, an approximate model is necessary to connect analytical far-field and near-field pressure solutions, eq. (19). The operating range of this connection is limited to the distance r = V t, where V is the constant plunging velocity, in front of the end of wet surface.

$$p_{far} = -\rho_f \frac{\Phi^{t_{j+\delta t_j}} - \Phi^{t_j}}{\delta t_j} - \rho_f \frac{\left(\text{grad}\Phi^{t_j}\right)^2}{2} \qquad (15)$$

$$p_{near} = \rho_f \frac{\dot{d}(t)^2}{2}\left(1 - \left(\frac{1-u}{1+u}\right)^2\right), \qquad u \in [0,1] \qquad (16)$$

where u is determined by the resolution of the non-linear system:

$$y - d(t) = \frac{\delta_{jet}}{\pi}\left(2\ln u - \frac{4}{u} - \frac{1}{u^2} + 5\right), \quad \text{for } y < d(t) \qquad (17.1)$$

$$y - d(t) = \frac{\delta_{jet}}{\pi}\left(-2\ln u - 4u - u^2 + 5\right), \quad \text{for } y > d(t) \qquad (17.2)$$

where $\delta_{jet} = \frac{\pi}{8}\frac{V^2 d(t)}{\dot{d}(t)^2}$ stands for the jet thickness. The connection between far-field and near-field pressures is achieved through the link pressure (p_{link}) and the corrected link pressure (p_{link}^c):

$$p_{link} = \rho_f \frac{V d(t)\dot{d}(t)}{\sqrt{2d(t)(d(t)-y)}} \qquad (18)$$

$$p_{link}^c = p_{link}, \quad \text{for } y < d(t) - r$$

$$p_{link}^c = p_{edfc} + \left(\frac{d(t)-y}{r}\right)^2 \left[p_{link}(d(t)-y) - p_{edfc}\right], \quad \text{for} \begin{cases} y > d(t) - r \\ y < d(t) \end{cases} \qquad (19)$$

The final pressure is given by the composite numerical corrected pressure:

$$p_{num}^f = p_{far} + p_{near} - p_{link}^c \qquad (20)$$

From these previous set of equations, we can find the maximal pressure p_{max}, as well as the pressure at the origin $y = 0$, p_{origin}.

$$p_{max} = p_{near}\big|_{u=1} = \rho_f \frac{\dot{d}(t)^2}{2} \qquad (21)$$

$$p_{origin} = p_{far}\big|_{y_0=0} = \rho_f V \dot{d}(t) \qquad (22)$$

The numerical evaluation of the far-field pressure requires, at each time increment Δt, two calculations of the velocity potential and a smaller time increment δt was used. Δt has been chosen constant and equals to $2\cdot10^{-5}$ s. The value of δt depends on the smallest mesh size M_s around the contact surface border and on the wet surface velocity $\dot{d}(t)$. On one hand δt must be greater than $M_s / \dot{d}$ to compute accurately the contact surface dimension. On the other hand, δt must be small enough to determine correctly the pressure field. Finally a value of $\Delta t/3$ was retained for δt. The Δt increment is also an important parameter for a good estimation by central differencing of $\dot{d}(t)$, eq. (23), and near-field pressure, eq. (16).

$$\dot{d}(t) = \frac{d(t_i) - d(t_{i-1})}{\Delta t} \qquad (23)$$

In this relation, $d(t_i)$ and $d(t_{i-1})$ are the wet surface distances calculated respectively at two consecutives increments t_i and t_{i-1} ($t_i - t_{i-1} = \Delta t$). That time increment is also very important for a correct simulation of the fluid-structure coupling in the deformable case.

We employ numerical iterations with a convergence criterion to obtain accurate values of the wet surface distances at every time increment, whereas the CASTEM approach uses a more approximate Wagner model. The convergence criterion is:

$$d_k - d_{k-1} \le \text{aprox.}2M_s \qquad (24)$$

To take into account the high potential gradient the zone located at the wet surface boundary was meshed with a very fine grid (fig. 2). First, the smallest mesh size M_s should be lower than the dimension of the physical singularity at the border of the wet surface. The jet thickness δ_{jet} is a good approximation of this dimension. Nevertheless, the smallest mesh size is

Copyright © 2008 by ASME

determined by the accuracy of $\dot{d}$, eq. (23), which strongly influences the quality of the pressure peak evaluation, eq. (21). We can estimate the logarithmic error of $\dot{d}$ as $\frac{\Delta\dot{d}}{\dot{d}} = \frac{M_s}{\dot{d}\,\delta t}$.

Knowing that $\dot{d} = \frac{\pi}{2}\frac{V}{\tan\beta}$ for wedges, we can prove in that case that the M_s equals to:

$$M_s = \frac{\pi}{2}\frac{V}{\tan\beta}\delta t\frac{\Delta\dot{d}}{\dot{d}} \qquad (25)$$

Choosing $\frac{\Delta\dot{d}}{\dot{d}} \le 10^{-2}$, for the least restrictive case ($V = 20\,m/s$ and $\beta = 6°$) we find $M_s \le 2$ µm, and for the most restrictive case ($V = 1\,m/s$ and $\beta = 14°$) we find $M_s \le 0{,}4$ µm. We finally chose the smallest mesh size M_s between 1 µm and 2 µm. It allows to verify the convergence criterion while keeping a reasonable computation time.

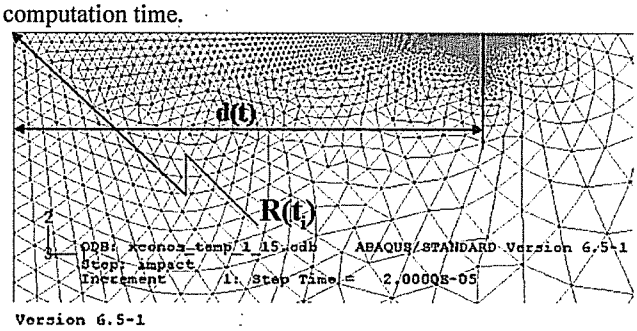

Figure 2 – Detail of fluid mesh

We optimized the fluid mesh reducing the number of elements successively while checking that the results still agreed with equations (21) and (22), respectively. We found numerically that the minimal number of elements is 11000. Despite these improvements, the computation times with ABAQUS remain superior comparatively to Impact++ CASTEM. The latter used only 1500 elements for the fluid mesh domain. The dimension of the meshed fluid zone is continuously adapted to the contact surface between solid and water ($R(t_i) = 8\,d(t_i)$). For a smaller value of $R(t_i)$, the total effort is overestimated especially at the onset of impact.

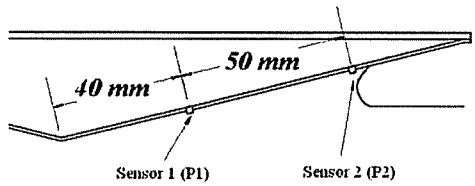

Figure 3 – Position of pressure sensors

In our simulations, only wedges and cones are analyzed. Three deadrise angles β (6°, 10°, and 14°) between the body and the calm water surface were considered. The pressure was measured at two points (P1 and P2), figure 3.

II.C. Rigid bodies

For the rigid cases, the velocity was assumed to be constant. This hypothesis allows to know the exact position of the body in water at every time increment. In our simulations, the maximum pressure values agree very well with those determined with CASTEM (fig. 4). We also obtain the same wet surface propagation velocity, as well as the resulting vertical force on the solid.

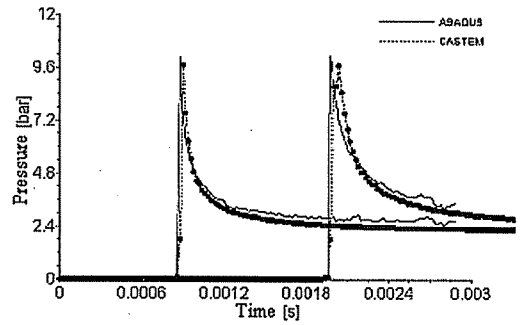

Figure 4 - Pressure vs. time at points P_1 and P_2 for wedge of 10° deadrise angle and 5 m/s impact velocity

The main difference between the two codes refers to the calculus of the wet surface extent d. Donguy used an analytical estimation, whereas we employed an iterative process with a convergence criterion. The results obtained with ABAQUS and CASTEM were also very similar and in good agreement with analytical solutions described by Wagner, Zhao and Faltinsen [6].

In conclusion, those satisfactory results have permitted to bring a first validation to our code and they allowed the continuation of the work in the deformable case.

II.D. Deformable structures

The study of impact with deformable structures is more complex. Indeed, a finite element method must be employed to obtain the shell evolution in parallel with fluid calculation.

Concerning this hydro-elastic coupling, two approaches for fluid-structure interaction have been implemented. The first one is based on an explicit resolution without global convergence criterion (ping-pong scheme), whereas the second (process scheme) is an implicit method associated with two global convergence criteria (strain energy for the structure and maximum peak pressure for the fluid). Donguy [5] employed an explicit iteration followed by only an implicit one at every time increment. His method can be considered as less accurate since no convergence criterion is enforced.

The boundary conditions for the structure are similar with those used by Donguy in his experiments. The extremities are modeled by two crosshead guides (fig. 5).

The left link stands for the symmetry of the problem. At the right link a constant velocity, equal to initial velocity of impact, is prescribed, whereas an initial velocity is prescribed at the rest of the solid.

Copyright © 2008 by ASME

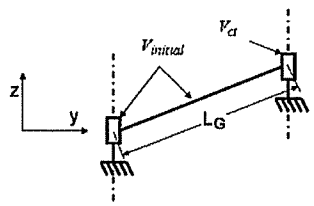

Figure 5 – Boundary and initial conditions for the structure

For the ping-pong scheme, the coupling is explicit since the constant pressure at t_i is applied for the dynamic solid simulation between t_i and t_{i+1} (fig. 6).

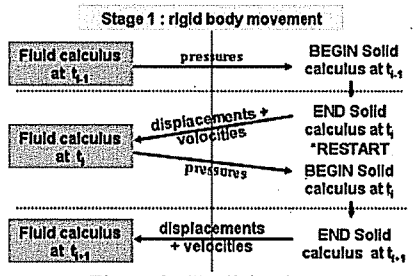

Figure 6 – Explicit scheme

For the solid calculation, the *Restart function of ABAQUS was employed to stop and restart the simulation without losing the history of positions, velocities and accelerations at nodes. This method does not represent a true improvement over Donguy's approach, but it allows us to obtain a first representation of the fluid-structure coupling.

The implicit scheme (fig. 7) is a real improvement of hydro-elastic fluid-structure coupling. The main idea is to calculate, alternatively up to the complete plunging of the structure into water the time history of displacement and velocity of the structure nodes and the fluid pressure time history along the contact surface for prescribed deformation.

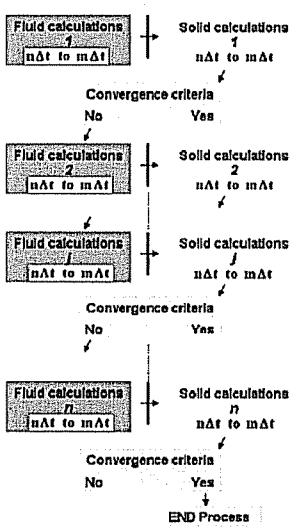

Figure 7 – Process scheme

This iterative process starts with the flow computation, considering a rigid body motion for the solid. The obtained fluid pressure time history along the contact surface is transferred to the transient dynamic finite element analysis of the structure. The post-processing of this finite element analysis allows determining the time history of displacement and velocity of the structure nodes which is transferred to the fluid finite element analysis, and so on. This iterative scheme, denoted here 'process scheme', is carried on until convergence.

The implicit feature of the fluid-structure coupling is justified by the fact that the constant pressure at time t_{i+1} (t_i with "ping-pong" scheme) is applied for the dynamic deformable structure simulation between t_i and t_{i+1}.

We conducted a first simulation of a deformable cone impacting the water surface achieving fluid and solid calculations coupled in an implicit manner over the total time of analysis. With this method CPU time becomes very long. For the improvement of the computing time we cut out the total time of analysis in great intervals of time (GIT). Then, we carry out calculation of process until convergence over each great interval of time. The last idea was to choose time increment Δt as a GIT.

We simulated the impact at 10 m/s of a 14° wedge (steel, 2 mm thickness, wedge meridian 128 mm long). For this example, we calculated the CPU time using different great intervals of time. We have obtained 80 hours for a GIT of $10\Delta t$ and 37.8 hours for a GIT of $1\Delta t$, respectively.

For this last case, we compared this approach to the ping-pong scheme and the Impact++ CASTEM procedure (fig. 8). The maximal discrepancy is around 10 % between our implicit coupling method and the Impact++ CASTEM results. Even if there is no reliable experiment to classify the different models, we consider that an implicit procedure with convergence criterion should be more appropriate than a simple approach (with a single explicit iteration followed by a single implicit iteration).

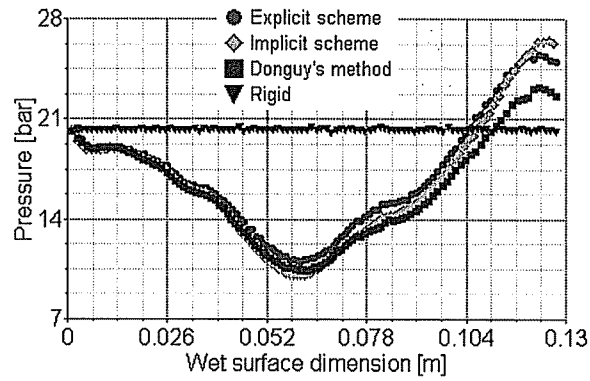

Figure 8 – Pressure peak evolution

For the two cases, rigid (eq. 26) and deformable (eq. 27), a verification of the mechanical energy conservation has been done. The mechanical energy balance provides good results. The relative error remains inferior to 1%.

$$P_{ext} = \dot{K}_e \tag{26}$$

$$P_{ext} + P_{int} = \dot{K}_e \tag{27}$$

In these relations, P_{ext} stands for the power of external forces, $\dot{K}_e$ the derivative of the kinetic energy (fluid + solid) and P_{int} is the elastic strain power of the structure. This calculus checks if the Neumann condition (no penetration) is correctly prescribed

Copyright © 2008 by ASME

along the contact line between solid and fluid. Indeed, using standard finite elements to mesh the fluid domain, around the contact surface border the vertical components of the heat gradient (temperature/velocity potential analogy) cannot be perfectly equal to the velocity of the structure.

III. SECOND APPROACH – ABAQUS/Explicit

III.A. NUMERICAL APPROACH

The second numerical approach is based on the use of the adaptive meshing technique available in the commercial finite element software ABAQUS/Explicit. The adaptive meshing technique combines the feature of pure Lagrangian analysis and pure Eulerian analysis. This type of technique is often referred to as Arbitrary Lagrangian-Eulerian (ALE) analysis. More details about ALE formulations can be found in [7].

Note that this approach has some advantages over the first one (Impact++). First, it is not restricted to moderate deadrise angles. Secondly, it allows to deals with 3D problems.

According to the ABAQUS documentation [7], flow modelling of compressible fluid can be achieved by using the linear U_s-U_p form of the Mie-Gruneisen equation of state. This equation defines the pressure as function of the density ρ and of the internal energy per unit mass E_m of the fluid::

$$p = f(\rho, E_m) \tag{28}$$

The equation for conservation of energy equates the increase in internal energy per unit mass, E_m, to the rate at which work is being done by the stresses and the rate at which heat is being added. In the absence of heat conduction the energy equation can be written as:

$$\rho \dot{E}_m = p\frac{1}{\rho}\dot{\rho} + \mathrm{tr}(S\dot{e}_d) + \rho\dot{Q} \tag{29}$$

where p is the pressure, S is the deviatoric stress tensor, $\dot{e}_d$ is the deviatoric part of strain rate, and $\dot{Q}$ is the heat rate per unit mass. Assuming that shear stresses are negligible and that there is no heat source, the internal energy can be eliminated from the above equations (28-29) to obtain a p versus ρ relationship. This equation is called the Hugoniot curve and is used in the definition of the Mie-Gruneisen equation of state (eq. 30):

$$p - p_H = \Gamma\rho(E_m - E_H) \tag{30}$$

where $p_H=f(\rho)$ is the Hugoniot pressure, $E_H=f(\rho)$ is specific Hugoniot energy, Γ is the Grüneisen rapport :

$$\Gamma = \Gamma_0\frac{\rho_0}{\rho} \tag{31}$$

Γ_0 is a material constant and ρ_0 is the reference density.

The U_s-U_p type of equation of state intervenes on the Hugoniot pressure given by:

$$p_H = \frac{\rho_0 c_s{}^2 \eta}{(1-s\eta)^2} \tag{32}$$

where η is the nominal volumetric strain, $\eta = 1-\rho_0/\rho$. c_s et s are two parameters. Note that c_s corresponds to the sound velocity at small nominal strains. With the above assumptions, the pressure in the fluid is given by the following relationship:

$$p = \frac{\rho_0 c_s{}^2 \eta}{(1-s\eta)^2}\left(1-\frac{\Gamma_0\eta}{2}\right) + \Gamma_0\rho_0 E_m \tag{33}$$

The deviatoric response of the fluid is defined by the classical Newtonian fluid model $S = 2m\hat{D}$, where S and $\hat{D}$ are respectively the deviatoric stress and rate-of-deformation tensors. m is the viscosity of the fluid. The dimension of the fluid domain is ten times bigger than the solid dimension. This choice is based on the Impact++ ABAQUS observations, when a smaller fluid domain generates numerical errors and overestimates the fluid pressure. Besides, in the present approach, the compressibility of the fluid is taken into account. Waves in compressible media travel at finite speed. Therefore, the pressure acting on the structure will not depend on the size of the fluid domain if the following condition is satisfied:

$$L \geq \frac{c_s T}{2} \tag{34}$$

where L is the minimal distance between the structure and the limits of the fluid domain. T is the time of the simulation. When the condition (34) is satisfied, shock waves, that are first generated by the impact of the structure and then reflected on the limits of the fluid domain, do not have time enough to come back to the structure.

The fluid domain consists of two zones. The first one corresponds to the area located near the surface of contact between the fluid and the solid. In this area, where the fluid undergoes severe deformation, a fine mesh of 4-node quadrilateral elements with bilinear interpolation functions and reduced integration (CPE4R in the case plane strain problems or CAX4R for axisymmetric problems) is used. The element size is about 150 µm. Besides, in order to prevent excessive mesh distortion, the adaptive meshing technique is used. The second zone, in which the deformation of the fluid remains moderate is modelled with a Lagrangian mesh of triangular linear elements (CPE3 or CAX3). In the proposed calculations, the number of elements varies from 70000 to 170000. Note that the CPE4R and CAX4R elements may suffer from hourglassing. Indeed, since these elements have only one integration point, it is possible for them to distort in such a way that the strains calculated at the integration point are zero, which, in turn, leads to uncontrolled distortion of the mesh. In order to prevent this phenomenon, these elements include hourglass control. For the calculations presented in this paper, an hourglass control, which combines a stiffness and viscous term, is used:

$$Q = \frac{1}{2}\left(Kq + C\frac{dq}{dt}\right) \tag{35}$$

where q is an hourglass mode, Q is the force (or moment) conjugated to q and K and Q are stiffness and viscous coefficients. The stiffness term acts to maintain a nominal resistance to hourglassing throughout the simulation, whereas the viscous term generates additional resistance to hourglassing under dynamic loading conditions.

Copyright © 2008 by ASME

Frictionless contact is used to model the interaction between the structure and the fluid. In the ABAQUS software, several methods are available for modelling the contact interface behavior. The first one is the "hard" contact model. In this case, the interface behaviour is defined by the impenetrability condition. This implies that no penetration is allowed between the surfaces. The contact interaction can be also modeled with a "softened" pressure-overclossure relationship, which leads to a regularization of the impenetrability condition. In the present study, the pressure-overclosure relation is prescribed by using an exponential law (fig. 9).

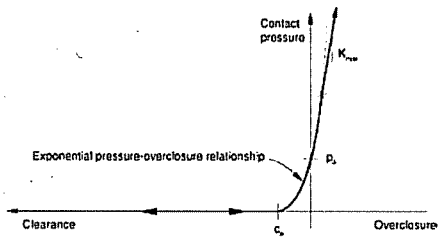

Fig. 9 – Exponential "softened" contact

This law depends on two parameters: c_0 and p_0. It has been observed that, concerning the hydrodynamic force, both the "hard" and the "softened" contact model yield similar results. Nevertheless, when the "hard" contact law is used, contact pressure distributions are very irregular. The results presented in this paper (fig. 10) have been obtained with the exponential "softened" contact model. Of course, the values of the parameters c0 and p0 should be carefully selected such that interpenetrations between the surfaces remain small. Constantinescu [8] have performed a parametric study of the effect of these parameters. He has observed that it is possible to obtain smooth solutions together with very small interpenetrations between the surfaces (of the order of 10 μm).

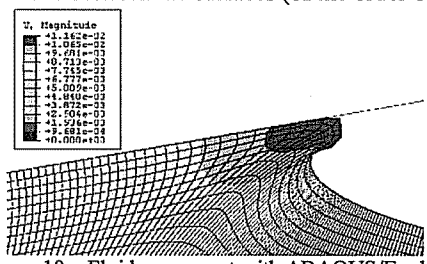

Figure 10 – Fluid movement with ABAQUS/Explicit

III.B. RESULTS FOR RIGID STRUCTURES

In ABAQUS/Explicit simulations, the fluid domain is fixed and the rigid structure impacts the free water surface at a constant velocity.

The 6.5 version of ABAQUS/Explicit has allowed us to obtain satisfactory results concerning the spatial and temporal pressure, and effort distribution for the rigid cases (wedges and cones) comparing with results issued from Impact++ ABAQUS and FLUENT codes.

The pressure peaks evolution of spatial distributions (fig. 11) is well reproduced regarding the Impact++ results.

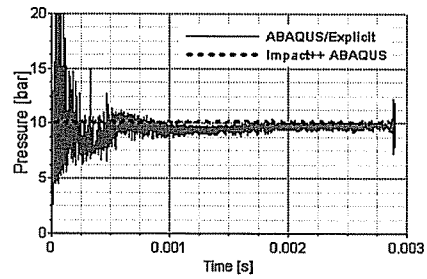

Figure 11 – Peaks pressure evolution for a rigid wedge
$\beta = 10°$, V = 5 m/s

We calculated the time histories of the pressure at two points P1 and P2 (according to figure 3). The results obtained with ABAQUS/Explicit are very close to those with FLUENT (fig. 12).

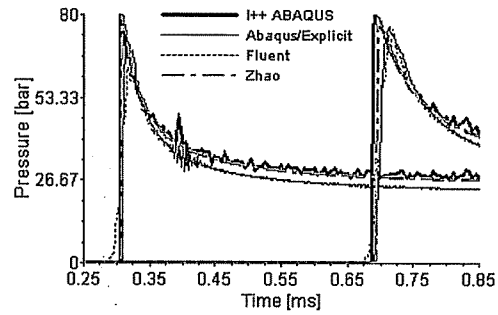

Figure 12 – Pressure vs. time at points P1 and P2 for wedge of 14° deadrise and impact velocity of 20 m/s

On the other hand, the Impact++ results are in good agreement with the theoretical model of Zhao and Faltinsen, where the maximal discrepancy between the two groups of results is around 10%. This difference can be explained by the geometric non-linearity used by ABAQUS/Explicit (explanation confirmed by the FLUENT calculations) in opposition to the Impact++ linearization. Concerning the wet surface propagation velocity, as we can see from the above figure, the four models forecast also very near values.

The main result for rigid wedges is the evolution of the non-dimensionalized expression f, eq. (36, associated to the force per unit length F which is function of time t, deadrise angle β, entry speed V and fluid density ρ_f.

$$f(\beta) = \frac{F \tan^2 \beta}{\rho_f V^3 t} \tag{36}$$

According to the figure 13, the hydrodynamic forces predicted by models based on Wagner's theory [Impact++ (for small deadrise angles β) and Zhao and Faltinsen analytical model] are higher compared to "non-linear" models [ABAQUS/Explicit, Fluent and Zhao and Faltinsen numerical model].

Copyright © 2008 by ASME

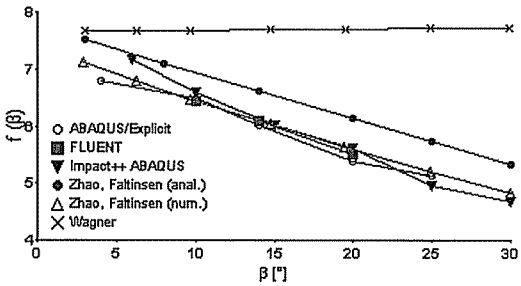

Figure 13 – Evolution of non-dimensionalized force function of deadrise angle in the case of the rigid wedges

For the rigid cone case, we found the observations similar to the wedges case. The ABAQUS/Explicit results are in good agreement with those of FLUENT. The hydrodynamic force predicted by Impact++ is slightly superior compared to Fluent and ABAQUS/Explicit results (fig. 14). There again, the discrepancy is also around 10%.

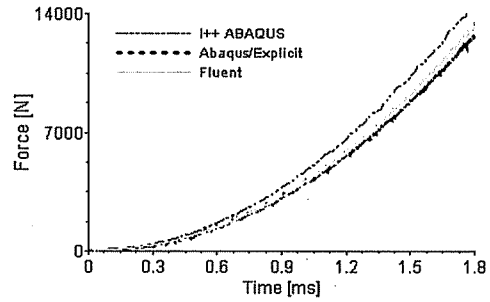

Figure 14 – Force vs. time for cone of 6° deadrise angle and impact velocity of 5 m/s

In this case, the pressure peaks (for the time histories of the pressure) at the points P1 and P2 occur a little earlier in the Impact++ simulations than in the others codes. It indicates that the wet surface propagation speed predicted by Impact++ is slightly more important than the one obtained with FLUENT and ABAQUS/Explicit.

IV. EXPERIMENTAL TESTS

In this part, the experimental tests conducted with a hydraulic shock press are presented. These tests were carried out in order to provide data to validate the previous numerical approaches. Firstly, we'll describe the main features of the shock machine and the experimental procedure. Secondly, the results for rigid bodies will be presented, and in the final subsection the comparisons with the numerical results will be shown.

IV.A. Experimental set-up

The experimental investigation consists of impact tests with simple structures using a hydraulic shock machine (fig. 15). This press allows to control the displacement and the impact velocity of the strikers. This machine is unique according to its performances and its flexibility (shock on water or solid crushing).

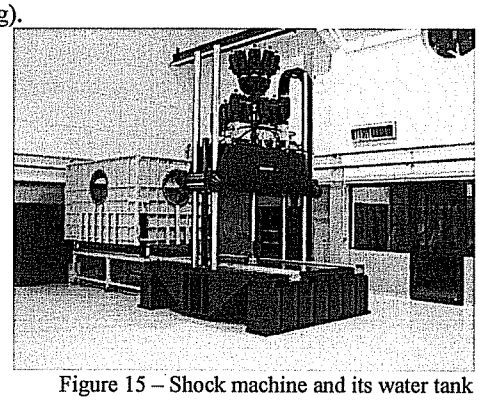

Figure 15 – Shock machine and its water tank

The tests campaign started with the impact of a rigid cone. The cone is fixed to the extremity of the machine piston through a specific part (fig. 16). The fluid tank is set under the shock device and is filled with 1.1 m height fresh water.

Figure 16 – Experimental setup of the rigid cone

The design of the cone must respect certain conditions. The first condition requires a minimal mass of the structure in order to limit the inertial forces. The impact force must be high enough in order to guarantee a satisfactory signal/noise ratio. The assumption of a rigid body should be assured by a very small overall deformation.

The cone diameter is related to tank water dimensions and equals to 330 mm. A 15° β deadrise angle has been chosen. In fact, this angle is important for an easier visualization of the free water surface motion with a high speed video camera. The optimal impact velocity is obtained using the non-dimensionalized force for cones, eq. (37). Thus, when the cone is entirely plunged, the impact force does not exceed the maximal pushing force of the machine. An Impact++ ABAQUS simulation allowed to evaluate the $\overline{F}(\beta = 15°)$ value. Finally, the constant impact velocity must be lower than 16 m/s.

$$\overline{F}(\beta) = \frac{F \tan^2 \beta}{\rho_f V^4 t^2} \qquad (37)$$

Copyright © 2008 by ASME

The cone diameter and deadrise angle being fixed, the cone height was determined with respect to a stiffness criterion so that the displacement of the cone extremity should be lower than the machining tolerance. The final dimensions of the aluminum alloy cone are presented on the figure 17.

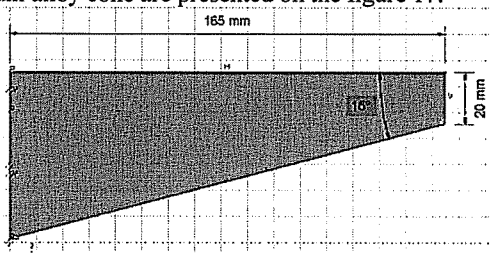

Figure 17 – Aluminum alloy cone dimensions

Displacement, force and acceleration measurements are performing during impact.

The piston displacement is measured by an internal machine sensor. The sampling frequency is 2500 Hz.

The impact force is measured by four KYOWA™ (model FFG-2-1K-C1-11) gauges located at 50 mm from the piston extremity, within a Wheatstone full bridge. The latter is connected to a NICOLET™ data acquisition system recording at a sampling rate of 5000 Hz.

The acceleration is measured with a piezoresistive sensor type EGA-125-100D. The electrical signal delivered by that sensor is recorded on the same system at the same sampling frequency. It allows to quantify the inertial forces due to slightly non constant velocity during the impact.

It is also important to detect correctly the contact between the cone and water. To solve the problem, we have used an electrical detection system. The NICOLET™ data acquisition system records the voltage in an electrical circuit that changes its impedance when the cone touches the water.

IV.B. Experimental results

The first tests were achieved using the rigid cone. The impact velocity was set to 15 m/s. At this speed, the experimental hydrodynamic force is around 90 kN, in good agreement with the numerical simulations. Moreover, the time evolution of the hydrodynamic force should be parabolic. Figure 18 showing the experimental time evolution of the hydrodynamic force confirms that theoretical result.

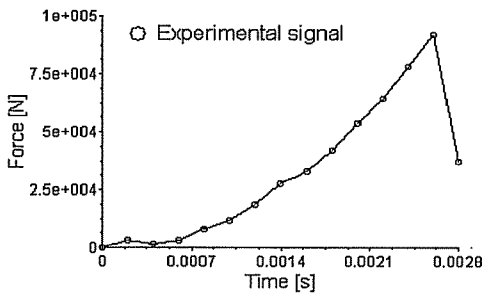

Figure 18 – Signal force

In addition to basic acquisition systems (force, displacement, acceleration), we also used a PHOTRON high speed digital video camera to record the evolution of the interaction between cone and water in a window of 1024x128 pixels at 15000 frames per second (fig. 19).

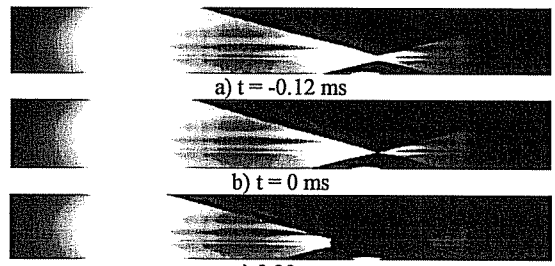

Figure 19 – Photos obtained during the impact of a 15° deadrise angle cone at 15 m/s

The impact duration is short, approximately 2.5 ms. We observe that the piston speed slightly fluctuates. Fortunately, this variation, less than 1%, remains small during the impact.

From the last measurements, we have determined the non-dimensionalized force $\overline{F}$, eq. (37). It represents the main parameter in order to validate the numerical simulations with experiments.

Figure 20 shows the evolution of $\overline{F}$ with time. The time t = 0 corresponds to the top of contact between cone and water, detected by the electrical system. In the first instants of plunging, $\overline{F}$ is not well calculated since the measured effort F and the time t are almost zero. Afterwards, $\overline{F}$ tends to an "asymptotic" value until the end of test (maximal impact force). Impact++ ABAQUS and experimental results for $\overline{F}$ are found to be in good agreement, although the force $\overline{F}$ is initially perturbed.

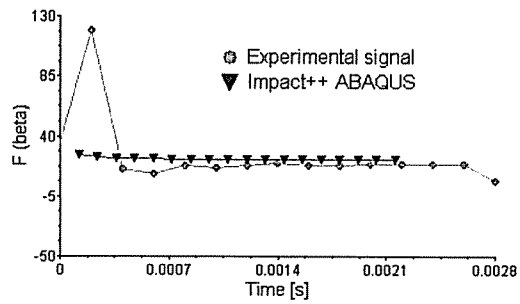

Figure 20 – Impact++ ABAQUS and experimental non-dimensionalized force $\overline{F}$

We have established the "asymptotic" value error with the logarithmic variation of eq. (37). This error is around 13%.

Table 1 gives experimental and numerical results for the rigid cone (β = 15, V = 15 m/s for tests 1 and 2 and β = 15, V = 12 m/s for test 3). These results are globally mutually in good agreement. The Impact ++ ABAQUS result is very close to the experimental values.

Copyright © 2008 by ASME

Test	1	2	3
Incertitude	13%	13%	11%
$\overline{F}$ experimental	**22.7 ± 3**	**22.0 ± 3**	**22.1 ± 3**
$\overline{F}$ Impact ++ ABAQUS	**22.7**		
$\overline{F}$ ABAQUS/Explicit	**23.4**		
$\overline{F}$ FLUENT	**23.4**		

Table 1 – Comparison between numerical and experimental results

V. CONCLUSIONS

In this paper, we presented two numerical approaches for solving two-dimensional slamming problems and an experimental work in order to validate these two numerical tools.

Firstly, we describe the fluid problem in terms of the velocity potential formulation, the asymptotic method was used to solve these equations. For the rigid body entry, the hybrid fluid-thermal approaches using CASTEM or ABAQUS FE codes give similar results for the propagation velocities of the wetted surface and approximately a 5% discrepancy for pressure. The maximum values of pressure calculated with ABAQUS are very close to those given with CASTEM. Both differ from Donguy's experimental values as the sensors average the pressure over the sensor area (around 5 mm diameter). Averaging our numerical results over the sensor area gives much better agreement with experiments (tab. 2).

Speed	2.5 m/s		5 m/s	
Position	P1	P2	P1	P2
Impact++ ABAQUS	**1.67**	**1.68**	**6.7**	**6.7**
CASTEM	**1.6**	**1.6**	**5.4**	**6.6**
Donguy's tests	**1.0**	**1.4**	**4.1**	**5.6**
ABAQUS averaged	**1.12**	**1.6**	**4.5**	**5.6**

Table 2: Pressures [bar] on rigid cone with a 10° deadrise angle

For the deformable structure case, differences between ABAQUS and CASTEM are larger, certainly related to the numerical modeling.

ABAQUS/Explicit model does not allow determining accurate pressure peaks values (fig. 11) without a very fine meshing and it is associated high CPU cost. But accurate reliable information is obtained for the resulting effort. In the first simulations the pressure and impact force still dependent on c_0 and p_0 coefficients of exponential "softened" contact. We also came across difficulties relating to excessive grid mesh distortions during the final phase of the simulation. Globally, the ABAQUS/Explicit results are in good agreement with Impact++ ABAQUS results and particularly with those of FLUENT. The study of slamming phenomenon with ABAQUS/Explicit seems to be a potential way, especially for the 3D cases. But previously it is necessary to carry out simulations with 2D deformable structures, paying a special attention to the fluid-solid contact treatment.

The last part of this paper dealt with experiments. It describes the experimental equipment, the choice of impacted structure and the instrumentation. These tests consist of impacting a rigid cone with a free water surface initially at rest. The experimental asymptotic value of the non-dimensionalized force $\overline{F}$ (eq. 37) is well-predicted by the numerical results. In conclusion, we appreciate that numerical results were well confirmed by these first experimental tests.

NOMENCLATURE

- T - temperature [m^2/s] or [m]
- Γ_L - free surface [m]
- Γ_B - vertical projection of the body wetted surface [m]
- Δt - numerical time increment
- Φ - velocity potential of fluid [m^2/s]
- Ψ - displacement potential of fluid [m^2]
- β - deadrise angle
- λ - thermal conductivity
- ρ_0 - initial fluid density [kg/m^3]
- ρ_f - fluid density [kg/m^3]
- c_s - sound speed in water [m/s]
- c_0 - clearance between fluid and solid [m]

ACKNOWLEDGMENTS

We are grateful for discussions and support to Volker Bertram (ENSIETA, Brest), Steven Kerampran for supplying numerical results with CDF code FLUENT, University of Liege for the Post-doctoral Fellowship and the Marstruct NoE – FP6 EU Project. The experimental study was supported financially by DGA/MRIS which we want to thank.

REFERENCES

[1] ISSC Committee, 1991, "Dynamic Loads Effects", Proceedings of the 11th International Ship and Offshore Structures Congress, Vol. 1, pp. 239-318;

[2] Langrand, B., Deletombe, E., 2001, "De la validité des comparaisons calculs/essais dans les problemes couplés fluide/structure", 15th French Congress of Mechanics, Nancy;

[3] Bertram, V., 2000, "Practical Ship Hydrodynamics", Butterworth+Heinemann Oxford;

[4] Wagner, H., 1932, "Über Stoss-und Gleitvorgänge an der Oberfläche von Flüssigkeiten", ZAMM, Vol. 12, pp. 193-215 ;

[5] Donguy, B., 2002, "Study of the fluid interaction structure at the time of the hydrodynamic impact", Ph. D. Thesis, ECN, Nantes, France;

[6] Zhao, R., and Faltinsen, O.M., 1993, "Water entry of two-dimensional bodies", Journal of Fluid Mechanics Vol.246, pag. 593-612;

[7] Hibbit, Karlsson, and Sorensen Inc., 2004, "ABAQUS Analysis User's Manual. Volume V: Prescribed Conditions, Constraints & Interactions";

[8] Constantinescu, A., 2004, "2D modeling of the impact of a body on water. Damage initialization", Ph.D. Thesis, Ensieta, Brest, France.

Copyright © 2008 by ASME